Inversion of Gravity Data to Define the Pre-Tertiary Surface and Regional Structures Possibly Influencing Ground-Water Flow in the Pahute Mesa—Oasis Valley Region, Nye County, Nevada

By T.G. Hildenbrand[1], V.E. Langenheim[1], E.A. Mankinen[1], *and* E.H. McKee[1]

Open-File Report 99-49
Version 1.0

1999

Prepared in cooperation with the
U.S. DEPARTMENT OF ENERGY
NEVADA OPERATIONS OFFICE
(Interagency Agreement DE-AI08-96NV11967)

Available online at http://wrgis.wr.usgs.gov/open-file/of99-49/

U.S. DEPARTMENT OF THE INTERIOR
U.S. GEOLOGICAL SURVEY

[1] 345 Middlefield Road, Menlo Park, CA 94025

TABLE OF CONTENTS

ILLUSTRATIONS

TABLE

ABSTRACT

A three-dimensional inversion of gravity data from the Pahute Mesa–Oasis Valley region reveals a topographically complex pre-Tertiary basement surface. Beneath Pahute Mesa, the thickness of the Tertiary volcanic deposits may exceed 5 km within the Silent Canyon caldera complex. South of Pahute Mesa in Oasis Valley, basement is shallower (< 1 km) but between this valley and the Timber Mountain caldera complex is a basin that probably represents, in part, a moat related to the Timber Mountain caldera complex. Of particular interest is a NE-trending lineament, named here the Thirsty Canyon lineament (TCL), separating terranes at significantly different elevations. Southeast of the TCL, a highly undulating basement surface descends deeply into several calderas, whereas NW of the TCL basement is relatively flat and shallow. Because as many as four calderas seem to abruptly terminate at the TCL, the TCL may reflect a major buried fault zone, which influenced caldera growth. This inferred Thirsty Canyon fault zone and several EW basement ridges in the derived 3-dimensional basin thickness model may influence the flow of ground water from the Pahute Mesa region to Oasis Valley.

INTRODUCTION

As a consequence of testing underground nuclear devices at the Nevada Test Site, highly toxic contaminants entered the ground water and are presently migrating south from Pahute Mesa (Laczniak and others, 1996). To investigate possible flow paths, geophysical data recently have been collected (McCafferty and Grauch, 1997; Mankinen and others, 1998; and Schenkel, 1998) to define structures down gradient from Pahute Mesa. In the present study, we expand on a previous regional geophysical study by Grauch and others (1999) and provide an analysis of gravity data leading to a three-dimensional view of the basement surface, defined here as the contact between pre-Tertiary rocks and younger rocks. To first order, gravity anomalies in the study area (Figures 1 and 2) reflect variations in the thickness of sedimentary and volcanic rocks above the denser pre-Tertiary rocks (e.g., Mesozoic granatoids, Paleozoic carbonates and siliceous rocks and Precambrian sedimentary and metamorphic rocks). Because the overlying Tertiary volcanic rocks are a principal aquifer lithology in the western Pahute Mesa–Oasis Valley region, their overall thickness provides important insights on structures possibly influencing ground-water flow. The resulting basement depth map was also important in siting ground geophysical surveys (Mankinen and other, 1999; Schenkel and others, 1999) for the purpose of providing greater details on interpreted geophysical features.

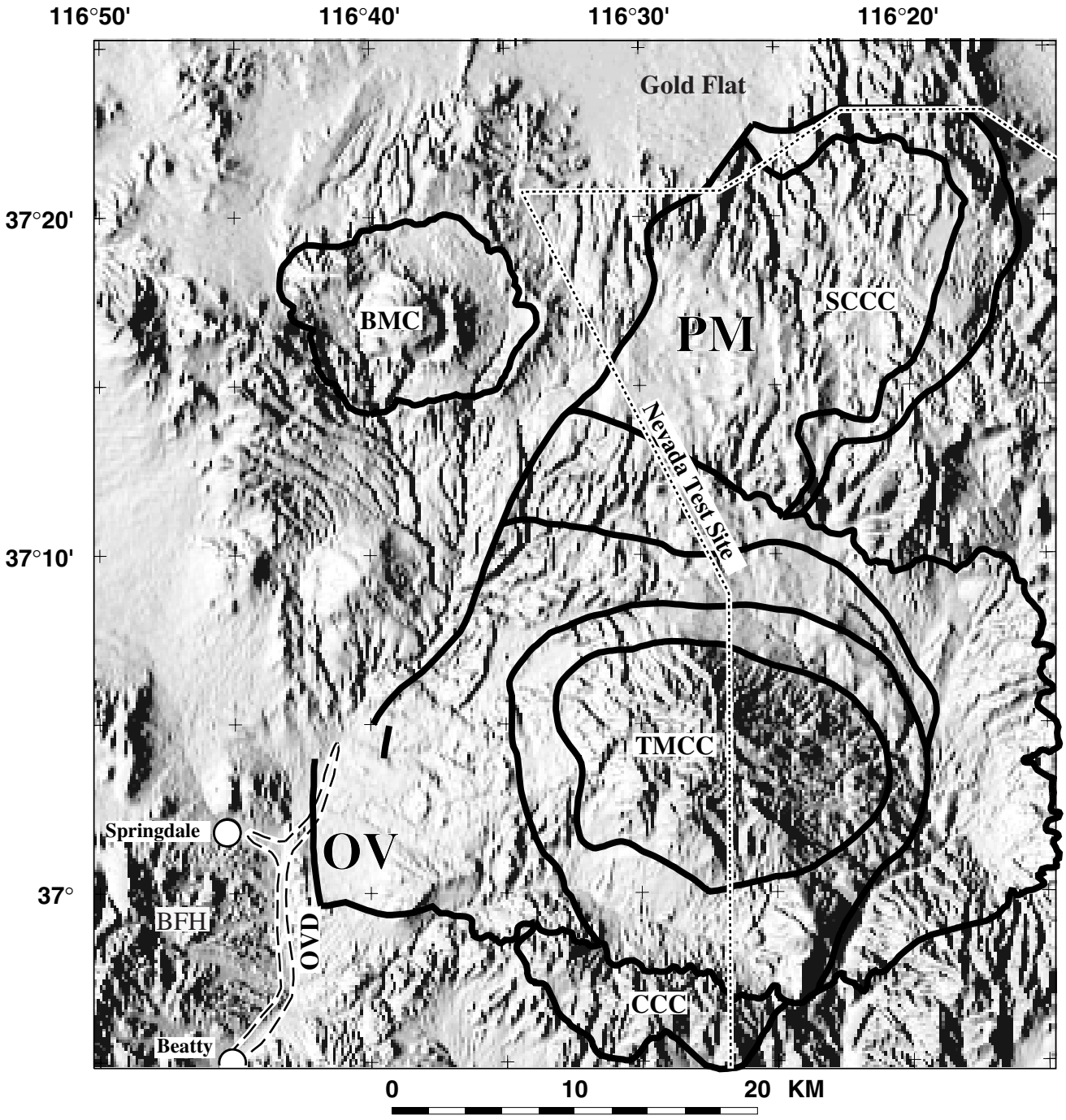

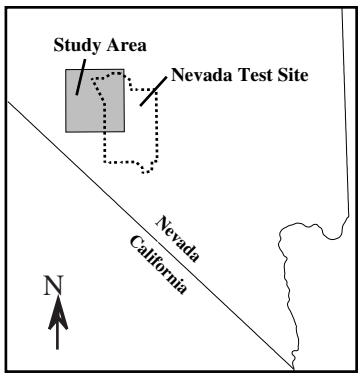

Figure 1. Topographic shaded-relief map of the Pahute Mesa (PM) and Oasis Valley (OV) region. Location of study area shown in inset. Black lines represent caldera structural boundaries as shown by Slate and others (1999), some based on this study. Letters denote: OVD–Oasis Valley water discharge area, CCC–Claim Canyon caldera, TMCC–Timber Mountain caldera complex, SCCC–Silent Canyon caldera complex, BMC–Black Mountain caldera, and BFH–Bullfrog Hills. Illumination is from the west.

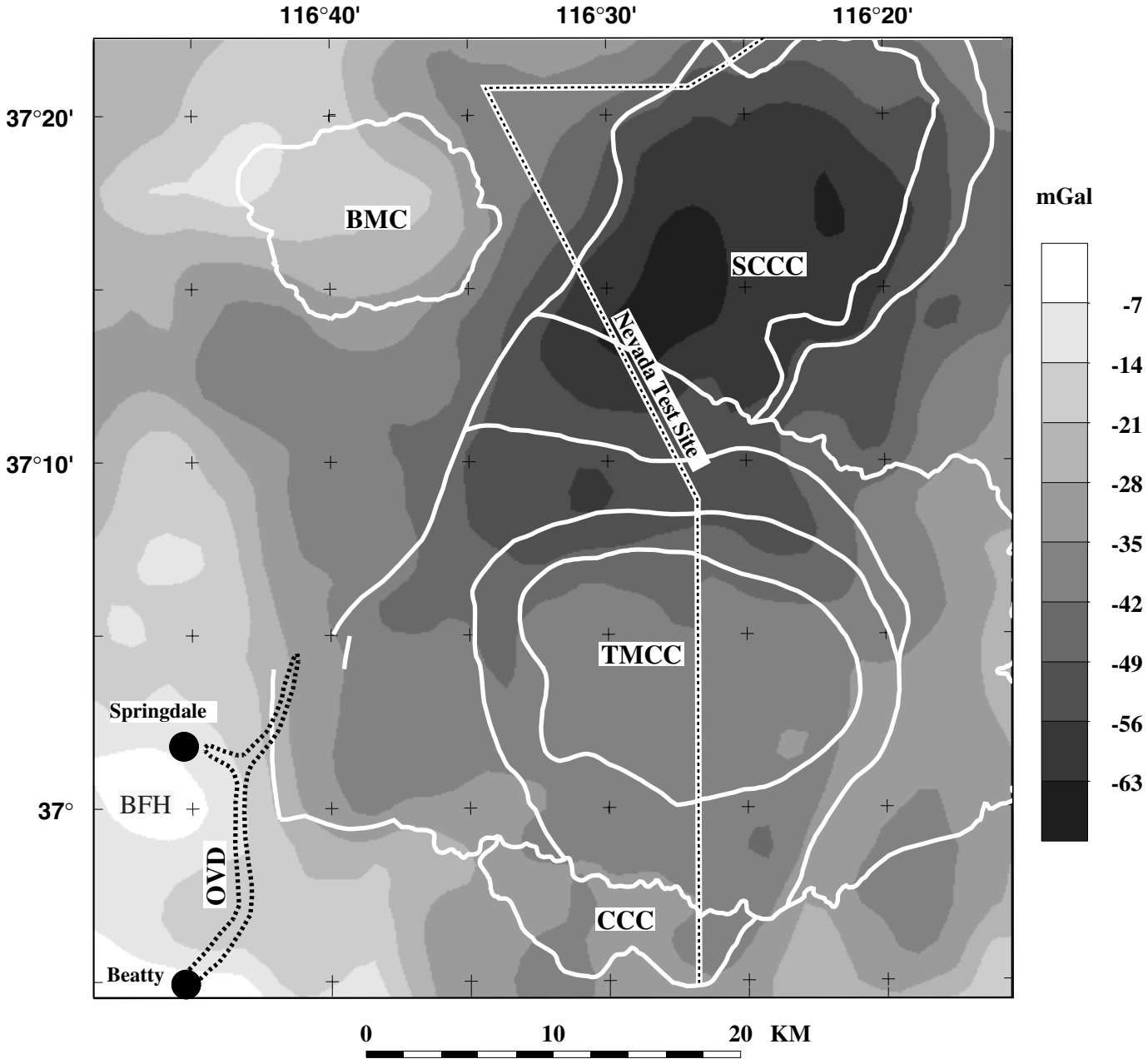

Figure 2. Isostatic residual gravity field of the Pahute Mesa-Oasis Valley region. Anomalies express to first order the average density of the middle and upper crust. Explanation of labels provided in Figure 1 caption.

ACKNOWLEDGMENTS

Discussions with Chris Fridrich, Gary Dixon, Tien Grauch and David Sawyer were important in formulating several of the conclusions of this paper. Bob Jachens and Pete Rowley, as reviewers and consulting colleagues, provided valuable suggestions related to both the technical and applied aspects of this study, leading to a greatly improved paper. Ward Hawkins, Bruce Hurley, Gail Palowski, Lance Protro, and Margaret Townsend also provided useful suggestions to improve the manuscript. We are grateful to Geoff Phelps for providing critical borehole gravity and digital geologic data. The Department of Energy through the Interagency Agreement DE-AI08-96NV11967 funded this project.

GEOLOGIC SETTING

The study area lies within the southern part of the Great Basin and includes the western part of the Nevada Test Site and the towns of Beatty and Springdale. In this area Precambrian crystalline rocks underlie a thick sequence (as much as 8 km) of late-Precambrian and Paleozoic sedimentary rocks. These rocks are intruded by Jurassic and Cretaceous granitic rocks, especially to the west near the California-Nevada border. Mesozoic compressional deformation produced folds and faults of all types, including regional thrust faults (Armstrong, 1968). Igneous activity in the study area was minor until Miocene time. In the Miocene (specifically 16-7 Ma) southwestern Nevada experienced pronounced volcanism over an area of >10,000 km^2, known as the SW Nevada volcanic field (Christiansen and others, 1977), where ash-flow tuffs and lava flows reach thicknesses locally of several kilometers (see results below). The Miocene ash-flow sheets and lava flows of the southwest Nevada volcanic field were deposited on the complexly deformed basement of Mesozoic granitic rocks and Paleozoic and Precambrian sedimentary and metamorphic rocks.

During the magmatic events in the Miocene, a series of overlapping calderas developed in the SW Nevada volcanic field that includes (from oldest to youngest) the Silent Canyon caldera complex, the Claim Canyon caldera, the Timber Mountain caldera complex, and the Black Mountain caldera (Nobel and others, 1991; Sawyer and others, 1994; Figure 1). It has been previously postulated that the Silent Canyon caldera complex consists of two nested calderas, the Grouse Canyon and the Area 20 calderas, spanning a time interval of 13.7 to 12.9 Ma (Minor and others, 1993; Sawyer and others 1994). The younger Area 20 caldera is not delineated by the gravity model presented here and it seems more likely that the Silent Canyon caldera complex consists of one caldera internally modified by a group of partially collapsed calderas. Our model suggests that to reconcile the great calculated thickness of the Tertiary volcanic rocks (locally > 5 km), many calderas must be nested to form the Silent Canyon caldera complex. The caldera boundaries shown in our figures are taken from

U.S. Geological Survey (1999). In this publication, the boundaries for the Silent Canyon caldera complex and the northern and western boundary of the Timber Mountain caldera complex are based largely on the results of this study.

The Timber Mountain caldera complex (about 11.4 to 10 my old) consists of the Rainier Mesa caldera and the smaller, nested Ammonia Tanks caldera (Figure 1). Sawyer and others (1994) hypothesized that the irregular outer boundary reflects the topographic margin of the Rainier Mesa caldera, the inner boundary is the structural margin of the Ammonia Tanks caldera and the two intervening partial boundaries represent the topographic margin of the Ammonia Tanks caldera. A relatively dense, shallow resurgent dome is associated with the Ammonia Tanks caldera and the younger (about 9 Ma) Black Mountain caldera.

The voluminous sheets of welded and non-welded ash-flow tuff and numerous lava flows erupting from volcanic centers associated with caldera structures and the calderas serve as major aquifers and confining units within the Pahute Mesa–Oasis Valley area (Laczniak and others, 1996). Thus knowledge of the thickness of the caldera fill and identification of caldera structures may be important in our understanding of the ground-water flow system. For example, a step or an abrupt shallowing of pre-Tertiary basement may represent a structural barrier channeling ground water and thus may result in a coinciding steep water gradient.

GRAVITY INVERSION

Methodology

The isostatic residual gravity field in Figure 2 is based on 3,526 existing gravity measurements (triangles, Figure 3; Harris and others, 1989) and 386 new gravity stations (solid circle; Mankinen and others, 1998). These new stations were collected along profiles crossing gravity features of interest to this study (discussed below). The overall distribution of gravity stations is about one station within 0.7 km^2 on the average. Although dense coverage exists within the Nevada Test Site, gravity stations are more widely spaced in other areas, such as north of Oasis Valley and in the Black Mountain area. Gravity data were reduced using the Geodetic Reference System of 1967 and referenced to the International Gravity Standardization Net 1971 gravity datum [Morelli and others, 1974; see also Mankinen and others (1998) for details on reducing the data to complete Bouguer anomaly values]. The isostatic residual anomaly was calculated using a reduction density of 2670 kg/m^3, crustal thickness of 30 km, and a mantle-crust density contrast of 350 kg/m^3 (see Simpson and others, 1986). All data were gridded at a spacing of 1 km using a minimum curvature algorithm of Webring (1982).

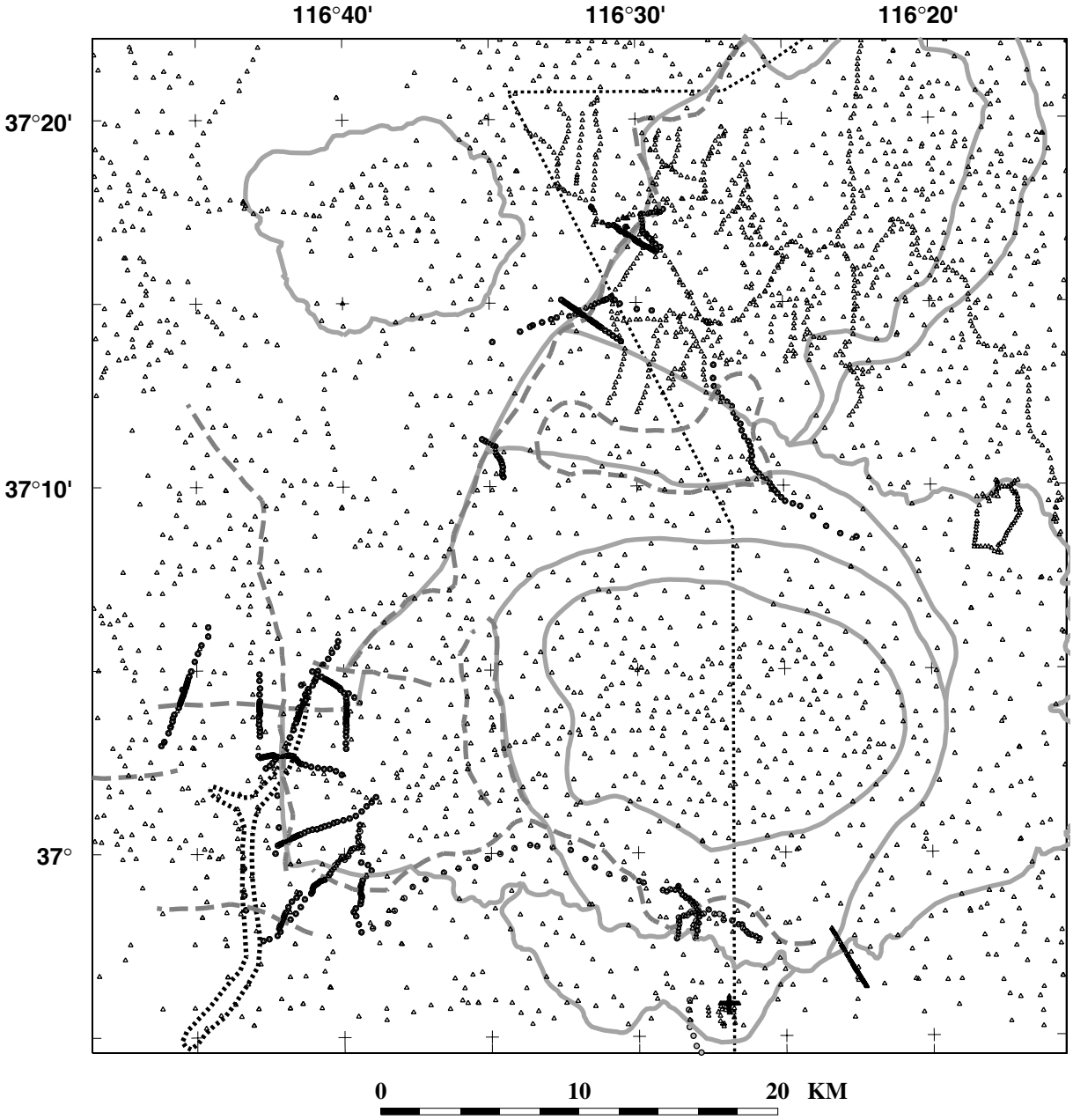

Figure 3. Location of gravity stations. Triangles denote existing stations and circles respresent stations acquired for part of this study (Mankinen and others, 1998). The new gravity data were collected along profiles primarily to better define regional gravity features, highlighted by the gray dashed lines.

To first order, the isostatic residual gravity field reflects the pronounced contrast between dense pre-Tertiary rocks (about 2670 kg/m^3) and significantly low-density volcanic caldera fill (Healey, 1968; Grauch and others, 1999). The gravity low over Pahute Mesa is one of the most prominent lows in western U.S., suggesting an unusually thick volcanic pile. Granitic resurgent domes (density about 2670 kg/m^3) under Timber Mountain and Black Mountain are the likely sources for the gravity highs (Kane and other, 1981; Grauch and others, 1999). Positive anomalies also occur over outcrops of relatively dense Paleozoic rocks in the Bullfrog Hills and west of Black Mountain (Figure 4; Wahl and others, 1997).

Using the gravity inversion method derived by Jachens and Moring (1990; modified to include drill hole data), we separated the isostatic residual anomaly into a basin field and a basement field. The basin gravity field reflects variations in the thickness of low-density Tertiary volcanic and sedimentary rocks. The basement gravity field reflects changes in density related to lithologic variations within the denser pre-Tertiary rocks. To reduce edge effects, the area over which the inversion was made extended beyond the area shown in Figure 4 (from lat. 36° 30' to 37° 30' and from long. 115° 52.2' to 117°).

In the inversion process, the density of basement is allowed to vary horizontally but the density of basin-filling deposits is fixed using a representative density versus depth relationship. Depths to basement based on well information constrain the calculations (Figure 4). Two wells just outside the study area helped constrain the results (well Ue25p1 shown in Figure 5 and a well at lat. 36 53.7° and long. -116 48.8° where basement was encountered at an elevation of 0.5 km). In this iterative approach, a first approximation of the basement gravity field is derived from those gravity measurements made on exposed pre-Tertiary rocks (Figure 4), augmented by appropriate basement gravity values calculated at sites where depth to basement is known and where variation of density with depth is assumed. This approximation (because the gravity effects of nearby basins are ignored) is subtracted from the observed gravity, which provides the first approximation of the basin gravity field. Using the assigned density-depth relation, the thickness of the basin-filling deposits is calculated. The gravitational effect of this first approximation of the basin-filling layer is computed at each known basement station. This effect is subtracted from the first approximation of the basement gravity field and the process is repeated until the change in basin thickness and thus basement gravity is negligible.

In the calculation of the complete Bouguer anomaly and the isostatic residual anomaly, the rock mass above the sea level was assumed to have a density of 2670 kg/m^3. This estimated reduction density is probably appropriate for areas where the near-surface layer consists chiefly of pre-Tertiary rocks (e.g., the

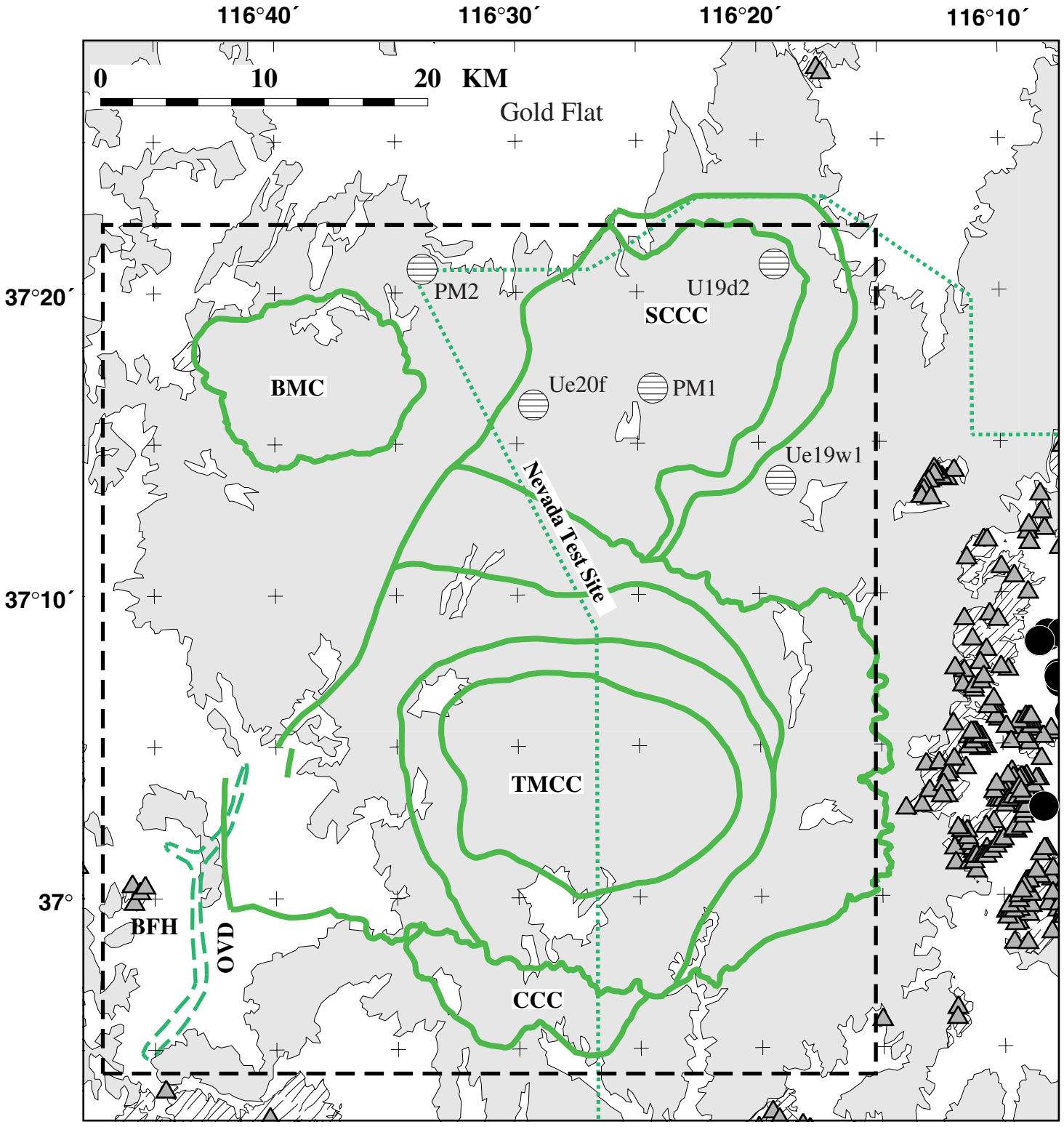

Figure 4. Generalized geology and basement control used in basin analysis. Heavy dashed rectangle is the present study area shown in the other figures. Labels explained in Figure 1 caption.

- Cenozoic sedimentary deposits
- Cenozoic volcanic rocks
- Pre-Tertiary basement rocks
- Drillhole where basement depth is known
- Drillhole where basement gravity is assumed (-10 mGal)
- Gravity station made on basement outcrop

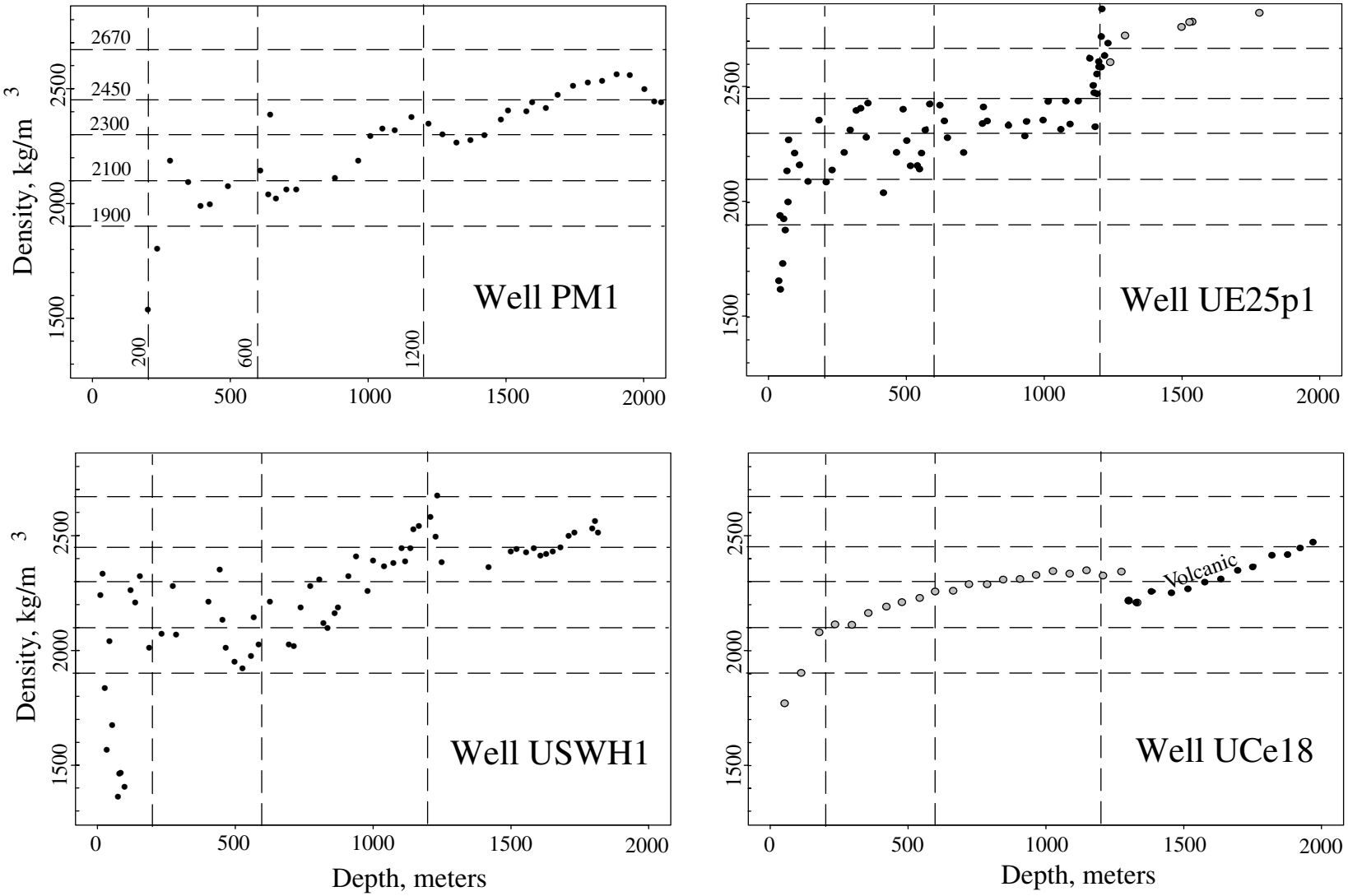

Figure 5. Borehole gravity data for 4 deep wells in or near the study area. The data show that density generally increases with depth. Well PM1 (Kososki and others, 1978) and USWH1 (Robbins and others, 1982) penetrate entirely volcanic rocks in the Silent Canyon caldera complex (lat. 37° 16', long. 116° 24') and at Yucca Mountain (lat. 36° 52', long. 116° 27'), respectively. Well UE25p1 (Healey and others, 1984) is also in the Yucca Mountain region (lat. 36° 50', long. 116° 25') but encountered Paleozoic rocks (denoted by the gray circles) below a thick volcanic section. North of the Nevada Test Site (lat. 38° 35', long. -116° 11.5') well UCe18 (Dixon and Snyder, 1967; Healey, 1967) sampled alluvium and lake sediments (gray dots) to a depth of about 1.3 km where intrusive rhyolite was encountered. In these wells, at a depth of between 1 and 2 km, density increases to about 2450 kg/m^3 in the volcanic rocks.

Bullfrog Hills). However, in areas of volcanic and sedimentary rocks in the near-surface layer (average density generally between 2100 and 2400 kg/m^3), the above basin analysis method will yield basin thicknesses that are too large. For example, the change in elevation between Pahute Mesa (where the average density of the rocks above sea level is roughly 2200 kg/m^3 as discussed below) and the Bullfrog Hills (where dense Paleozoic rocks are exposed) is about 800 m. The anticipated overestimate in basement depth or basin thickness, related to an erroneously high reduction density at Pahute Mesa, is roughly 1,000 m (3,000 ft).

Density-depth Function

The accuracy of the thickness results is highly dependent on the assumed density-depth relation of the Tertiary rocks and the initial density assigned to basement rocks. The Tertiary rocks are almost entirely of volcanic origin (although thin alluvial deposits are found throughout the study area, Figure 4). Complicating this task of selecting representative densities at a particular depth is the significant variation in density related to the degree of welding and alteration of the ash-flow tuffs, to structure (e.g., landslides and shallow, dense volcanic domes), and to water saturation. Because density generally increases with depth due to compaction, a layered density model is assumed for the Cenozoic deposits, although the lenticular nature of the volcanic rocks is acknowledged.

The uppermost, unsaturated layer contains the lowest densities. Bulk overburden densities in 55 shallow (~ 600 m) wells from the Pahute Mesa region average 1970 kg/m^3 (R.G. Warren, LANL, written commun., 1998; URL http://queeg.ngdc.noaa.gov/seg/geochem/swnvf/). From rock samples, Snyder and Carr (1984) measured densities of sediment (alluvium) ranging between 1600 and 2000 kg/m^3 and of volcanic rocks ranging between 1700 and 2300 kg/m^3. We assume a density of 1900 kg/m^3 in the top 200 m.

At depth, selected densities are based on deep-borehole gravimeter studies in the region of the southwest Nevada volcanic field (e.g., Figure 5) and borehole density logs from deep wells in the Pahute Mesa region (e.g., PM-1, PM-2 and UE20f, Figure 4; see Mankinen and others, 1999). A well (UCe18) considerably north of Pahute Mesa (lat. 38° 35') was used to investigate reasonable densities within alluvium at depths greater than 200 m. At depths between 1,000 and 2,000 m, the data reveal that the density of the volcanic rocks on average increases to 2450 kg/m^3. This density increase reflects, in part, the depth at which pressure and temperature have depleted most of the porosity to the degree that the geologic processes (e.g., welding and alteration) causing major density variations at shallower depths are considerably less of a factor. We assume that the density of rock between 1,200 m and the depth of basement is 2450 kg/m^3.

In the depth range from 200 to 1,200 m, density is highly variable although the relation of increasing density with increasing depth is generally observed. Based largely on borehole gravity studies, we define two intervening layers (Figure 5): 200 to 600 m—2100 kg/m3 and 600 to 1,200 m—2300 kg/m3.

The final density-depth relation of the Cenozoic basin fill is shown in Table 1. It should be noted that a more careful review of published data leads to a similar density-depth relation (Mankinen and others, 1999; Phelps and others, 1999). Although in this relation we adopted the same depth intervals of Jachens and Moring (1990) used in compiling a Nevada Cenozoic basin thickness map, our discrete vertical density distribution (1900, 2100, 2300 and 2450 kg/m^3) is somewhat lighter than the ones used by them for exposed volcanic rock (2220, 2270, 2320 and 2420 kg/m^3) and sedimentary rock (2020, 2120, 2320 and 2420 kg/m^3). Due to the limited area of the present study, the density data suggest that a single density-depth function can adequately represent terranes with both volcanic and sedimentary rocks at the surface.

Alternative density-depth models were considered and are shown in Table 1. Within a caldera, the existence of thick, low-density tuff layers cannot be ignored, particularly beneath Pahute Mesa. Borehole gravimeter studies in the Silent Canyon caldera complex (Ferguson and others, 1994; R.G. Warren, LANL, written commun., 1998) reveal densities of 2100 kg/m^3 extending in many areas to depths of over 1,000 m. In such situations calculated basement depths will be overestimated. On the other hand, a locally thick, shallow layer or dome of densely welded tuffs would lead to underestimated basin thicknesses. To understand the possible effects of different density-depth functions, alternative depth-density functions were investigated (Table 1). Although locally large discrepancies in calculated thickness arise (discussed below), the average basement depth in the final model differs little with those of the alternative models (differences of +0.7 km to –0.5 km, Table 1).

Results

The present basin analysis separates the isostatic residual gravity field (Figure 2) into a basement component (Figure 6) and basin component (Figure 7). The basement gravity field provides information on lateral changes in basement rock types. The regional basement gravity lows in the central and northwestern parts of the study area probably reflect basement densities of roughly 2670 kg/m^3 related either to resurgent granitic intra-caldera intrusions that underlie Black Mountain and Timber Mountain or to thick Paleozoic to late Precambrian shale and quartzite. The increase in the regional gravity field in the eastern part of the study area may be due to more or thicker carbonate units. Generally carbonate rocks are slightly denser than the siliceous rocks. Directly south of Beatty the increase in basement gravity probably reflects the dense metamorphic Precambrian rocks of the Pahrump Series (Hamilton, 1988), with an average laboratory density of about 2740 kg/m^3.

Table 1. Density-depth functions used to determine the thickness of basin-filling deposits.

Depth Range	Density (kg/m^3) for 3 models		
	Final	Low-density	High-density
0 – 200 m	1900	1800	2000
200 – 600 m	2100	2000	2300
600 – 1,200 m	2300	2100	2300
>1,200 m	2450	2300	2450
	Basin Thickness (mean ± standard deviation)		
	2.2 ± 1.5 km	1.5 ± 1.3 km	2.7 ± 2.0 km

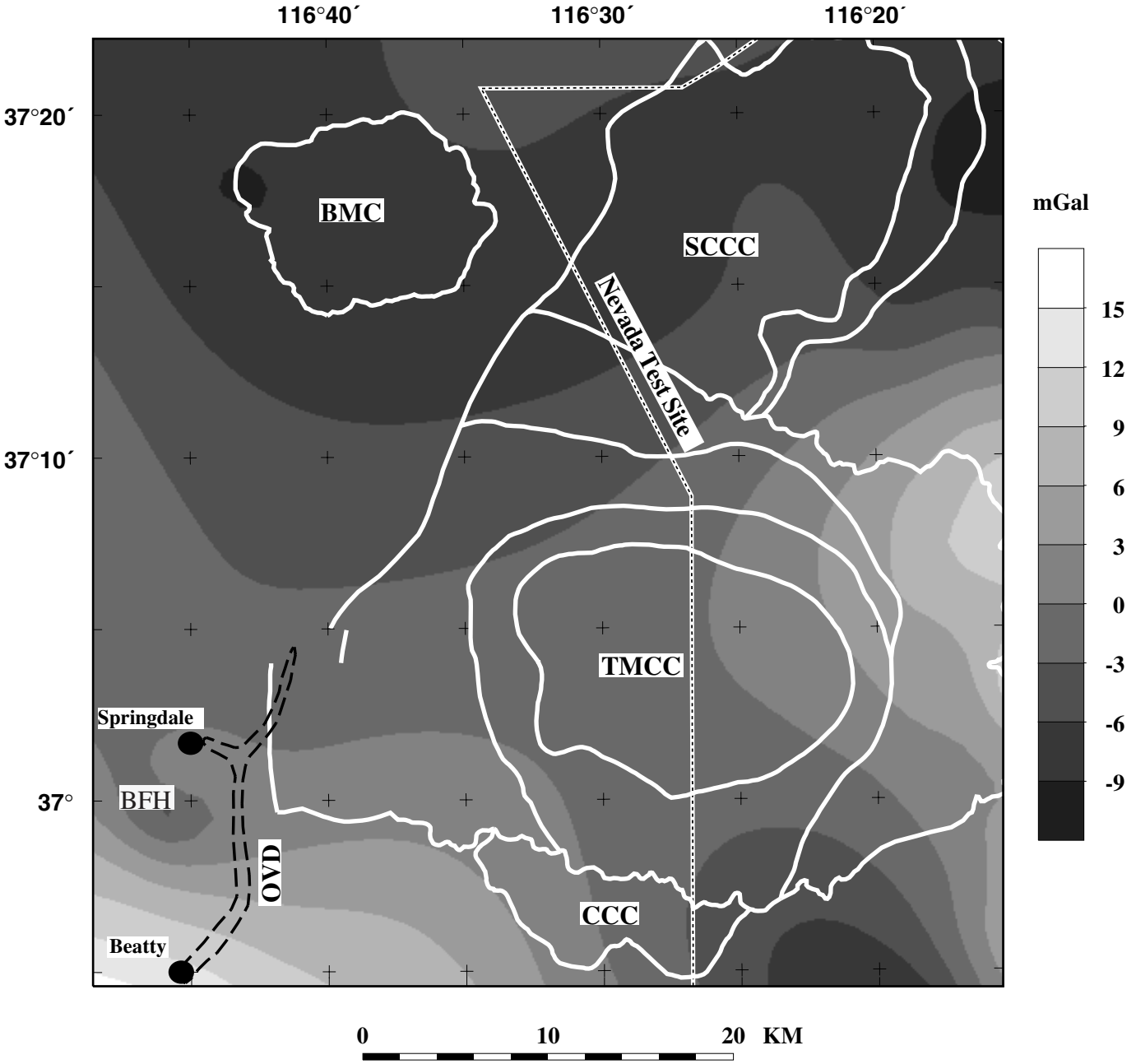

Figure 6. Gravity anomalies caused by basement rocks as derived from the inversion of the gravity measurements. These anomalies added to the basin anomalies shown in Figure 7 will produce the original gravity field in Figure 2. Explanation of labels is provided in Figure 1 caption.

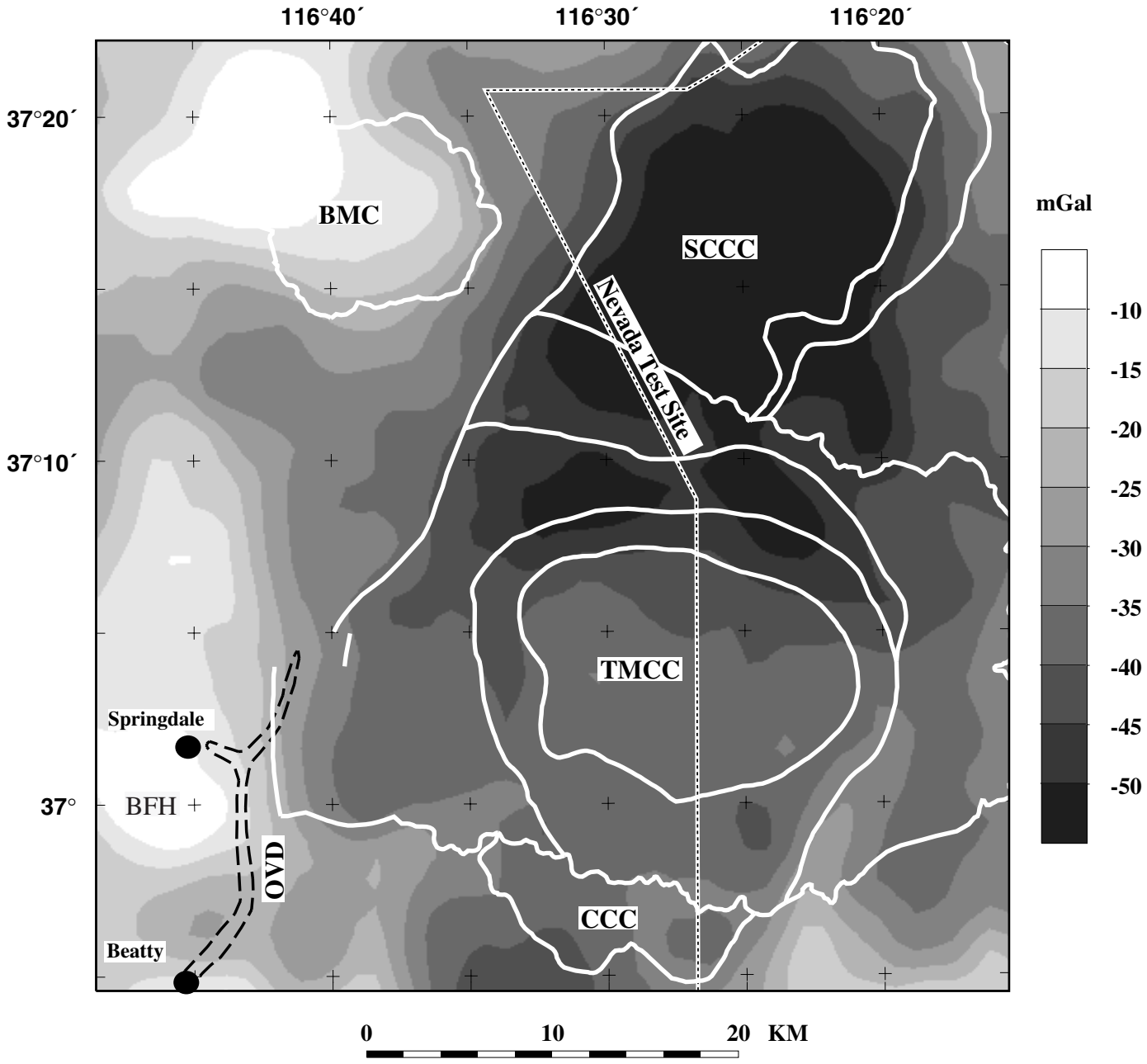

Figure 7. Basin gravity anomalies as derived from the inversion of the gravity field. Explanation of labels is provided in Figure 1 caption.

Using the selected density-depth function, the inversion of the basin gravity field (Figure 7) provides the thickness of the low-density Cenozoic sedimentary and volcanic layers shown in Figure 8. Subtracting these thicknesses from the topographic elevations yields a three-dimensional view of the pre-Tertiary basement surface (Figure 9). In general basement is shallower outside the caldera systems along the western and southern parts of the study area. Basement descends to great depths beneath the Silent Canyon caldera complex. The resurgent domes of the Black Mountain caldera and the Timber Mountain caldera complex are clearly expressed as elliptically shaped basement highs.

The limitations of these results vary. In regions where basement control exists (either from basement outcrops or well data, Figure 4) the results are probably good (e.g., the southwestern and eastern parts of the study area). The lack of control over a large area, from Pahute Mesa to Oasis Valley, prompted us to constrain depth estimates by assigning basement gravity values at five locations in the region of the Silent Canyon caldera complex (Figure 4). These five sites are optimally distributed and are the locations of deep wells where the geology at depths greater than 2 km is known. The selected value (-10 mGals) for basement gravity forced the computed basement anomaly (Figure 6) over this caldera to be similar to those over the Black Mountain and Timber Mountain calderas. In other words, we assume basement geology and thus associated density to be similar beneath the calderas within the study area. This approach to constraining the basin thickness results in a mean calculated basement depth of 4.5 km ± 2.0 km in the Silent Canyon caldera region. Without the inclusion of these basement gravity estimates, basement in this region increases to a mean depth of 6.3 km ± 2.5 km.

The uncertainty in the density-depth function poses problems elsewhere in the study area. The Oasis Valley basin, which is east of the Oasis Valley water discharge area, changes in average thickness by about –1 km and +0.9 km using the lighter and denser density-depth functions (Table 1), respectively. In addition, intense local gravity anomalies might delineate structures with densities deviating greatly from the assumed density-depth relation. Two prominent peaks in the basement surface (highlighted with "?" in Figure 8) could, for example, be related to volcanic domes of flow rock at the margin of the Silent Canyon caldera complex or, less likely, to shallow structural domes of densely welded tuff. If these shallow, dense (> 2450 kg/m^3) sources are present, the actual basement would lie at greater depths.

The variability in local density-depth functions and the lack of basement control in some areas (particularly between Pahute Mesa and Oasis Valley) strongly argue

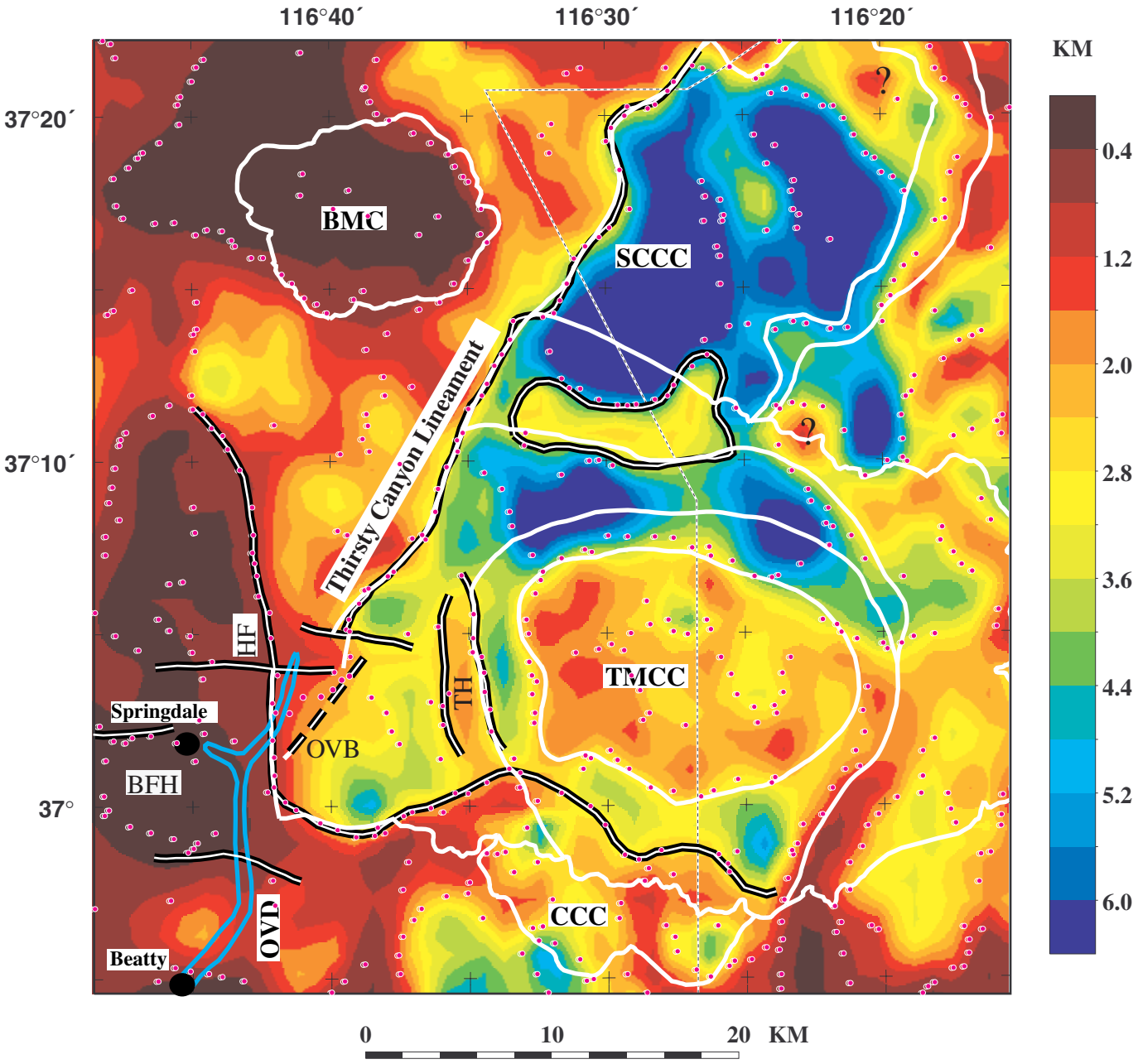

Figure 8. Thickness of Cenozoic deposits based on the inversion of gravity data. Magenta circles define boundaries across which density varies (i.e., the maximum magnitude of the horizontal gradient of the isostatic gravity field; Blakely and Simpson, 1986). Inferred density boundaries are shown by the black/white lines (dashed segment may be the SW extension of the Thirsty Canyon lineament). Two shallow peaks in basement near the NE and SE boundary of the Silent Canyon caldera complex (highlighted with "?") may reflect shallow domes of densely welded tuffs. The Oasis Valley basin, Hogback fault and Transvaal Hills are located with "OVB", "HF" and "TH", respectively. Explanation for the remaining labels is provided in Figure 1 caption.

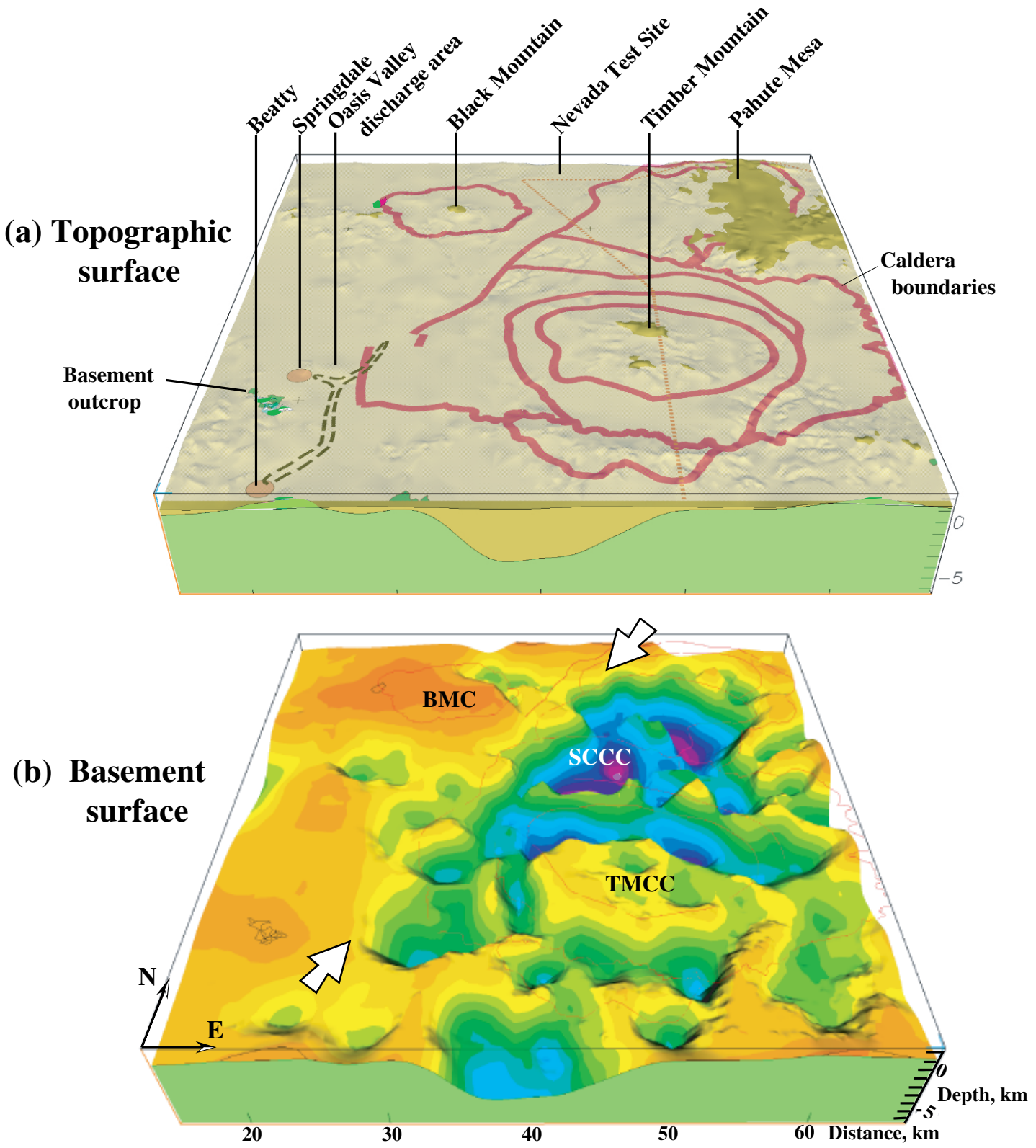

Figure 9. Three-dimensional view of the subsurface beneath Pahute Mesa and Oasis Valley. (a) Topographic surface. Transparent plane at an elevation of 1.8 km shows cultural boundaries. Thus, mountains at elevations greater than 1.8 km pierce the sheet, such as Pahute Mesa. Gray dots show basement depth control. Green areas locate basement outcrops. (b) Basement surface. Shallow basement and deep basement are represented by the warm and cool colors, respectively. No vertical exaggeration. Arrows highlight the inferred Thirsty Canyon fault, expressed as a boundary separating terranes at different basement elevations.

that the relative change in basin thickness rather than its magnitude should be stressed in studying the basement surface in the Pahute Mesa–Oasis Valley region.

DISCUSSION

With these limitations of results in mind, we discuss the complex nature of the basement surface, clearly evident in Figures 8 and 9. Major interpreted basement boundaries are highlighted on Figures 8 and 10. Although many of these boundaries appear in previous publications as lineaments or near-surface features (e.g., Grauch and other, 1999; C.J. Fridrich, U.S. Geological Survey, written commun., 1998; Kane and others, 1981), Figures 8 and 9 provide greater details on the nature of basement related to these known features. The apparent NE-trending boundary lying along the northwest flanks of the Silent Canyon and Timber Mountain caldera complexes, first pointed out by Grauch and others (1999), is named here the Thirsty Canyon lineament (TCL). The TCL and inferred caldera structures are investigated below with particular attention given to their possible influence on ground-water flow. More detailed discussions on the geometry, depth and thus geohydrologic importance of some of these structures are provided by Mankinen and others (1999) and Schenkel and others (1999).

Caldera Structures

The thickness map appears to be a viable tool for identifying the major caldera structural margins formed during caldera collapse. A distinction is observed between caldera ring faults and associated topographic margins related to landslides, slumping and erosion of the structural margin which lie outboard from the major ring faults formed during caldera subsidence. For example, the outer boundary of the Silent Canyon caldera complex (outer white line, Figure 8) lies outside of the area of the thickest caldera-filling volcanic pile and thus it is the topographic boundary distant from the major caldera structural ring faults. The major offsets related to the structural margin, however, lie near the inner boundary of the Silent Canyon caldera complex.

In the western U.S., few gravity lows have magnitudes as great as the pronounced low over the Pahute Mesa region and assumed to be related to the Silent Canyon caldera complex (about 60 mGals; Figure 2; see Simpson and others, 1986). The resulting thick pile (locally > 5 km) of low-density volcanic rocks (mostly tuff), bordered by steep structural boundaries (some exceeding 45° dip), seems extremely thick. However, this conclusion is unavoidable unless one or two (or both) general geologic situations apply. First, basement under Pahute Mesa (Silent Canyon caldera complex) may be significantly less dense than 2670 kg/m^3. Based on the anticipated rock types and mineralogies, low-density basement rocks should occur only if they possess significant pore spaces.

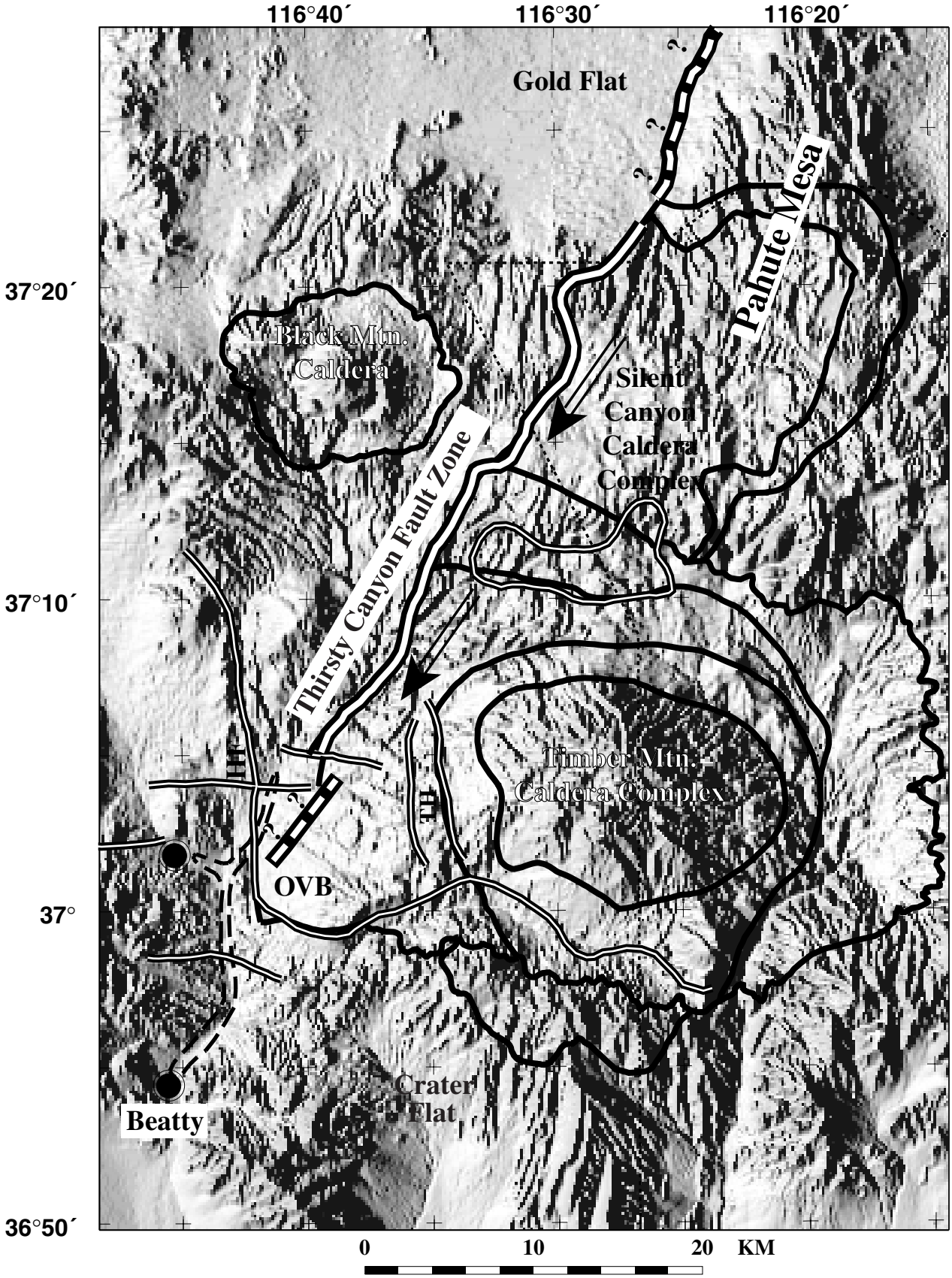

Figure 10. Major basement features (heavy black/white lines) interpreted from basin analysis. Dashed heavy black/white lines with "?" are the possible NE and SW extensions of the Thirsty Canyon fault. Heay black lines are caldera boundaries taken from Slate and others (1999). Arrows highlight the possible deflection of ground water along the Thirsty Canyon fault zone. The Oasis Valley basin, Hogback fault and Transvaal Hills are located with "OVB", "HF" and "TH", respectively.

It is doubtful that porosity is high at the expected basement depths (> 4 km). In addition, widespread hydrothermal alteration related to magmatic activity would likely result in the pore spaces being filled. Second, a thick low-density non-welded tuff layer may be present throughout the caldera complex. To reduce the thickness of the caldera fill to about 3 km, the density of the rocks above basement must be significantly reduced (e.g., 2100 kg/m^3 to basement depths). As discussed above, the data from wells in the Nevada Test Site area suggest an increase in density below 1 to 2 km. Moreover, like the basement rocks, porosity at depth (> ~ 2 km) is expected to be low (IT Corp, 1996) because of overburden pressure and alteration-related vein filling. On the other hand, if one selects the light density-depth model (Table 1), basement in the deep parts of the Silent Canyon caldera complex would be estimated to be roughly 1.5 km shallower than that shown in Figure 8 (~ 6 km). In summary, it seems unlikely that either an unusually low-density basement (say <2600 kg/m^3) underlies the caldera complex or a thick low-density volcanic layer exists at depth (say rock of density of 2100 kg/m^3 overlying basement). Our conclusions are supported by the identified rock types (John, 1995) and densities (David John, U.S. Geological Survey, written commun., 1998) associated with tilted late Oligocene caldera systems (> 4 km thick) in the Stillwater caldera complex in west-central Nevada.

To the south, the Timber Mountain caldera complex consists of the Rainier Mesa caldera and the younger Ammonia Tanks caldera (Figure 1). The thickness of the volcanic pile in the northern moat of the Rainier Mesa caldera is substantially greater than the moat thickness elsewhere, suggesting that voluminous sheets of volcanic rocks erupting from the Silent Canyon caldera complex underlie the northern Rainier Mesa moat (Kane and others, 1981). Other explanations for the deepening of basement are possible, such as the asymmetrical collapse of the Timber Mountain caldera complex. The outer boundary of the Timber Mountain caldera complex boundary (white line in Figure 8) is shown as a topographic margin whose northern part is north of an east-west basement ridge at about lat. 37° 11' N. This basement ridge is probably within the structural margin of either the Silent Canyon caldera complex or the Rainier Mesa caldera. The ridge is interpreted as dense intrusions penetrating ring faults and thus basement may not be as shallow as indicated in Figure 8. An alternative interpretation is that the ridge reflects dense moat-filling lava. The southern boundary of the Rainier Mesa caldera is an irregular boundary extending WNW to the Transvaal Hills, which probably represents the Ammonia Tanks caldera boundary (C.J. Fridrich, U.S. Geological Survey, written commun., 1998).

Oasis Valley Basin

The basement high underlying the Transvaal Hills has a steep eastern margin but a gently dipping western margin. The steep eastern edge is consistent with the

interpretation that the basement ridge is a caldera boundary. The gently dipping western margin of this ridge supports existing geologic models (C.J. Fridrich, U.S. Geological Survey, written commun., 1998) which show the basin west of this ridge is a half graben. The western margin of the basin (C.J., U.S. Geological Survey, written commun., 1998) is the steeply dipping Hogback fault, a prominent NS boundary apparent in the basin thickness map (Figures 8 and 9).

The southern boundary of the Oasis Valley basin is also clearly defined in the basin thickness map. The inferred average thickness of the sedimentary and volcanic rocks filling the basin ranges from 2.8 to 3.7 km (the mean depths derived from the light and dense models in Table 1, for the area from lat. 37° to 37 4' N and long. 116° 41' to 116° 36' W). The southern boundary of Oasis Valley basin is an EW-trending accommodation zone separating terranes with different structural styles (C.J. Fridrich, U.S. Geological Survey, written commun., 1998).

Thirsty Canyon Fault Zone

Grauch and others (1999) identified a NE-trending gravity gradient flanking the western sides of the Silent Canyon and Timber Mountain caldera complexes. The source of this gravity feature, here called the Thirsty Canyon lineament (TCL, Figure 10), is an abrupt change in depth of the basement surface (Figures 8 and 9). Ferguson and others (1994) also observed an abrupt thickening of the volcanic units along a profile crossing this lineament along the western margin of the Silent Canyon caldera complex.

Southeast of the TCL, the average thickness of Cenozoic beds increases to about 3 km, reflecting the thick caldera-filling volcanic units. It appears that the boundary, in part, possibly representing edges of at least 4 calderas, defines a major NE-trending structural break in the basement. It would seem to be fortuitous that the basement depth change related to the TCL occurs along a 40-km-long linear segment without some guiding structural control. In this area, the development of basin and range structures (< 17 Ma) resulted in NE- and NW-striking faults. Thus we propose that the TCL reflects a NE-trending basement fault, named here the Thirsty Canyon fault zone, that existed prior to the Miocene magmatic activity and that inhibited or influenced caldera growth. In other words, the vertical stresses arising during caldera subsidence were accommodated by the existing deep faults within the inferred Thirsty Canyon fault zone. Thus we define the Thirsty Canyon fault zone as the proposed ancestral basin and range fault and the overlying ring fractures related to the calderas that it bounds. U.S. Geological Survey (1999) accept our interpretation that the source of the Thirsty Canyon lineament influenced caldera growth and have shown this lineament (Figure 1) as the western boundary of the Silent Canyon and Timber Mountain caldera complexes.

If the Thirsty Canyon fault zone is extended farther to the NE, it is subparallel to the western edge of Pahute Mesa north of the Silent Canyon caldera complex (Figure 10). Here the inferred extension of the Thirsty Canyon fault is buried beneath thin alluvial deposits on Gold Flat. To the south, the Thirsty Canyon fault may terminate at an east-west ridge in the basement surface (lat. 37° 4' N). At this same latitude in Oasis Valley there exists an east-west gravity feature (Mankinen and others, 1999) and a coinciding northward step change in stratigraphic thickness (C.J. Fridrich, U.S. Geological Survey, written commun., 1998). This basement ridge and the east-west structures in Oasis Valley may delineate an accommodation or transverse zone separating terranes with different structural styles due to different tectonic stresses (C.J. Fridrich, U.S. Geological Survey, written commun., 1998).

The Thirsty Canyon fault zone may also continue along trend beneath the complex detachment structures in the Oasis Valley region or it may be offset left laterally as shown in Figure 8. Because the Thirsty Canyon fault zone is interpreted to represent the NW boundary of calderas to the north, we prefer that the inferred Thirsty Canyon fault zone continues SW to also represent the westernmost extent of the Timber Mountain caldera complex. Thus we would extend the previously assumed western margin of the Timber Mountain caldera complex (Minor and others, 1993) west to the Hogback fault, an interpretation also shown in existing geologic models (C.J. Fridrich, U.S. Geological Survey, written commun., 1998). Nobel and others (1991) extended this margin farther west than shown here, to a location west of Oasis Valley.

Hydrologic Implications

Laczniak and others (1996) showed that ground water is migrating southward from Pahute Mesa to Oasis Valley. Several flow paths are being investigated. Because one proposed path trends SW to Oasis Valley, the effect of the inferred Thirsty Canyon fault zone on ground-water flow must be investigated. As part of this study, we carried out detailed gravity (Mankinen and others, 1999; Figure 3) and magnetotelluric surveys (Schenkel and others, 1999) crossing the Thirsty Canyon fault zone. The reader is referred to these more thorough discussions on the hydrologic implications associated with the Thirsty Canyon fault zone and other basement structures. Here we only point out major basement structures (Figure 8) in the area between Pahute Mesa and Oasis Valley and highlight possible relations to flow paths.

The basement gravity field in Figure 6 may convey information on basement lithology. The gravity high east of the Timber Mountain caldera complex presumably reflects a thicker section of permeable, dense carbonate rocks (generally about 2700 kg/m^3 or greater). The gravity high in the vicinity of

Beatty delineates the dense, less permeable metamorphic Precambrian rocks of the Pahrump Series (Hamilton, 1988), with an average density of about 2740 kg/m^3. In the gravity inversion process, the basement gravity field over the Silent Canyon caldera complex was forced to have low intensities (~ 10 mGal). We propose that the basement gravity lows over the remaining parts of the study area reflect primarily Cenozoic granitic intrusions and fine-grained siliceous Paleozoic and Precambrian rocks such as argillite and quartzite (with densities about 2670 kg/m^3). These fine-grained rock types tend to impermeable.

Thus the abrupt rise in the relatively impermeable basement surface along the TCL strongly suggests that the inferred Thirsty Canyon fault zone represents a barrier to the deeper ground-water flow system and may channel ground water SW to the Oasis Valley discharge area. Shallow basement and numerous springs occur at the intersection of the Thirsty Canyon fault zone and the northernmost part of the Oasis Valley. The shallow ground water system above basement may be affected by the Thirsty Canyon fault zone due to shallow faulting. Heavily faulted zones, such as transverse zones, are known to be both barriers to flow across them and conduits to flow parallel with them (Rowley, 1998). However, rock alteration (Schenkel and others, 1999) above basement along the Thirsty Canyon fault zone may seal the faults. Thus the rocks above the Thirsty Canyon fault zone may act as a barrier or a conduit to ground-water flow, depending upon the effect of alteration on the porosity of the presumably heavily-fractured rocks.

Along this proposed southwestward flow path lie two EW basement ridges at 37° 11' and 37° 4'. For all three density-depth models in Table 1, these ridges lie at depths of about 3 km, suggesting that they will have minimal affect on the flow of ground water through most of the vertical extent of the main aquifer regime. On the other hand, these EW structures are probably fault-bounded ridges and the faults that may propagate upward and structurally affect the main aquifers and thus ground-water flow.

The rise in the basement surface along the southern boundary of the Oasis Valley basin might suggest a reduction of transmissivity for ground water flowing southward. Although much of the water flowing from Pahute Mesa may discharge in Oasis Valley, the southward path of the water is unknown. It may flow southwest toward the Beatty area or south into the Crater Flat region.

CONCLUSIONS

Basin analysis based on gravity data helps define three-dimensional structures beneath the alluvium and volcanic cover in the Pahute Mesa-Oasis Valley region. The observed complex nature of the basement surface leads to insights on caldera and fault structures that possibly influence ground-water

flow. In particular, an inferred NE-striking fault zone, the Thirsty Canyon fault zone, may represent a barrier or conduit to ground water, channeling ground water to the Oasis Valley discharge area. Pertinent future research should include the effects on ground-water flow of the shallow basement along the EW-trending southern boundary of the Oasis Valley basin. Such a study would provide new insights on whether ground water flows from Oasis Valley south toward Beatty or Crater Flat.

REFERENCES

Armstrong, R.L., 1968, Sevier orogenic belt in Nevada and Utah: Geological Society of American Bulletin, v. 79, p. 429-459.

Blakely, R.J., and Simpson, R.W., 1986, Locating edges of source bodies from magnetic and gravity anomalies: Geophysics, v. 51, p. 1494-1496.

Christiansen, R.L., Lipman, P.W., Carr, W.J., Byers, F.M., Jr., Orkild, P.P., and Sargent, K.A., 1977, The Timber Mountain-Oasis Valley caldera complex of southern Nevada: Geological Society of America Bulletin, v. 88, p. 943-959.

Dixon, G.L., and Snyder, R.P., 1967, Preliminary lithology and physical properties data, drill hole Ue18, Hot Creek Valley, central Nevada: U.S. Geological Survey Technical Letter, Central Nevada-2, May 1, 1967, 5 p.

Ferguson, J.F., Cogbill, A.H., and Warren, R.G., 1994, A geophysical-geological transect of the Silent Canyon caldera complex, Pahute Mesa, Nevada: Journal of Geophysical Research, v. 99, p. 4323-4339.

Grauch, V.J.S., Sawyer, D.A., Fridrich, C.J., and Hudson, M.R., 1999, Geophysical framework of the southwestern Nevada volcanic field and hydrogeologic implications: U.S. Geological Survey Professional Paper 1608 (in press).

Hamilton, W.B., 1988, Detachment faulting in the Death Valley region, California and Nevada: in, Carr, M.D., and Yount, J.C., eds., Geologic and Hydrologic Investigations of a Potential Nuclear Waste Disposal Site at Yucca Mountain, Southeastern Nevada: U.S. Geological Survey Bulletin 1890, p. 51-86.

Harris, R.N., Ponce, D.A., Healey, D.L., and Oliver, H.W., 1989, Principal facts for about 16,000 gravity stations in the Nevada Test Site and vicinity: U.S. Geological Survey, Open-File Report 89-682A, 78 p.

Healey, D.L., 1967, Borehole gravity meter observations in drill hole Uce-18, Hot Creek Valley, Nye County, Nevada: U.S. Geological Survey Technical Letter, Central Nevada-11, Special Projects Branch, 11 p.

——, 1968, Application of gravity data to geologic problems at Nevada Test Site, *in* Eckel, E.B., ed., Nevada Test Site: Geological Society of America Memoir 110, p. 147-156.

Healey, D.L., Clutsom, F.G., and Glover, D.A., 1984, Borehole gravity meter surveys in drill holes USW G-3, and UE-25p#1, Yucca Mountain Area, Nevada: U.S. Geological Report 84-672, 16 p.

IT Corporation, 1996, Regional geologic model documentation package: Prepared for DOE, Las Vegas, Nevada.

Jachens, R.C., and Moring, B.C., 1990, Maps of the thickness of Cenozoic deposits and the isostatic residual gravity over basement for Nevada: U.S. Geological Survey Open-File Report 90-404, 15 p.

John, D.A., 1995, Tilted middle Tertiary ash-flow calderas and subjacent granitic plutons, southern Stillwater Range, Nevada—Cross sections of an Oligocene igneous center: Geological Society of America Bulletin, v. 107, n. 2 p. 180-200.

Kane, M.F., Webring, M.W., and Bhattacharyya, B.K., 1981, A preliminary analysis of gravity and aeromagnetic surveys of the Timber Mountain area, southern Nevada: U.S. Geological Survey, Open-File Report 81-189, 40 p.

Kososki, B.A., Robbins, S.L., and Schmoker, J.W., 1978, Principal facts for borehole gravity stations in test well Ue19z, exploratory drill hole PM-1, and water well 5a, Nevada Test Site, Nye County, Nevada: U.S. Geological Survey Open-File Report 78-983, 16 p.

Laczniak, R.J., Cole, J.C., Sawyer, D.A., and Trudeau, D.A., 1996, Summary of hydrogeologic controls on ground-water flow at the Nevada Test Site, Nye County, Nevada: U.S. Geological Survey Water-Resources Investigations Report 96-4109, 59 p.

Mankinen, E.A., Hildenbrand, T.G., Dixon, G.L., McKee, E.H., Fridrich, C.J., and Laczniak, R.J., 1999, Gravity and magnetic study of the Pahute Mesa and Oasis Valley region, Nye County, Nevada: U.S. Geological Survey Open-File Report 99-303, 57 p.

Mankinen, E.A., Hildenbrand, T.G., Roberts, C.W., and Davidson, J.G., 1998, Principal facts for new gravity stations in the Pahute Mesa and Oasis Valley areas, Nye County, Nevada: U.S. Geological Survey Open-File Report 98-498, 14 p.

McCafferty, A.E., and Grauch, V.J.S., 1997, Aeromagnetic and gravity anomaly maps of the southwestern Nevada volcanic field, Nevada and California: U.S. Geological Survey Geophysical Investigations Map GP-1015, scale 1:250,000.

Minor, S.A., Sawyer, D.A., Wahl, R.R., Frizzell, V.A., Schilling, S.P., Warren, R.G., Orkild, P.P., Coe, J.A., Hudson, M.R., Fleck, R.J., Lanphere, M.A., Swadley, W.C., and Cole, J.C., 1993, Preliminary geologic map of the Pahute Mesa 30' x 60' quadrangle, Nevada: U.S. Geological Survey, Open-File Report 93-299, scale 1:100,000.

Morelli, Carlo, Gantar, C., Honasala, Taunao, McConnel, R.K., Tanner, J.G., Szabo, Bela, Uotila, U.A., and Whalen, G.T., 1974, The International Gravity Standardization Gravity Net 1971 (I.G.S.N. 71): Paris Bureau Centrale de l'Association Internationale de Geodesie Special Publication 4, 193 p.

Nobel, D.C., Weiss, S.I., and McKee, E.H., 1991, Magmatic and hydrothermal activity, caldera geology, and regional extension in the western part of the southwestern Nevada volcanics field: in, Raines, G.L., Lisle, R.E., Schafer, R.W., and Wilkinson, W.H., eds., Geology and Ore Deposits of the Great Basin, Geological Society of Nevada, Reno, Nevada, p. 913-934.

Phelps, G.A., Langenheim, V.E., and Jachens, R.C., 1999, Thickness of Cenozoic deposits of the Yucca Flat, Nevada Test Site, Nevada, inferred from gravity data: U.S. Geological Survey Open-File Report 99-310, 29 p.

Robbins, S.L., Schmoker, J.W., and Hester, T.C., 1982, Principal facts and density estimates for borehole gravity stations in exploratory wells Ue4ah, Ue7j, Ue1h, Ue1q, Ue2co, and USW-H1 at the Nevada Test Site, Nye County, Nevada: U.S. Geological Survey Open-File Report 82-277, 20 p.

Rowley, P.D., 1998, Cenozoic transverse zones and igneous belts in the Great Basin, western U.S.—Their tectonic and economic implications, in Faulds, G.E. and Stewart, J.H., eds., Accommodation Zones and Transfer Zones—The Regional Segmentation of the Basin and Range Province: Geological Society of America Special Paper 323, p. 195-228.

Sawyer, D.A., Fleck, R.J., Lanphere, M.A., Warren, R.G., Broxton, D.E., and Hudson, M.R., 1994, Episodic caldera volcanism in the Miocene southwestern Nevada volcanic field: Revised stratigraphic framework, $^{40}Ar/^{39}Ar$ geochronology, and implications for magmatism and extension: Geological Society of America Bulletin, v. 106, p. 1304-1318.

Schenkel, C.J., 1998, Magnetotelluric data in the Pahute Mesa and Oasis Valley areas, Nye county, Nevada: U.S. Geological Survey Open-File Report 98-504, 70 p.

Schenkel, C.J., Hildenbrand, T.G., and Dixon, G.L., 1999, Magnetotelluric study of the Pahute Mesa and Oasis Valley regions, Nye County, Nevada: U.S. Geological Survey Open-File Report 99-355, 46 p.

Simpson, R.W., Jachens, R.C., Blakely, R.J., and Saltus, R.W., 1986, A new isostatic residual gravity of the conterminous United States, with a discussion of the significance of the isostatic residual anomalies: Journal of Geophysical Research, v. 91, p. 8348-8372.

Snyder, D.B., and Carr, W.J., 1984, Interpretation of gravity data in a complex volcano-tectonic setting, southwestern Nevada: Journal of Geophysical Research, v. 89, p. 10,193-10,206.

U.S. Geological Survey, 1999, Digital geologic map and database of the Nevada Test Site and vicinity, Nye, Lincoln, and Clark Counties, Nevada, and Inyo County, California: U.S. Geological Survey Open-File Report (in press).

Wahl, R.R., Sawyer, D.A., Minor, S.A., Carr, M.D., Cole, J.C., Swadley, W.C., Laczniak, R.J., Warren, R.G., Green, K.S., and Engle, C.M., 1997, Digital geologic map of the Nevada Test Site area, Nevada: U.S. Geological Survey Open-File Report 97-140, scale 1:120,000.

Webring, Michael, 1982. MINC--A gridding program based on minimum curvature: U.S. Geological Survey Open-File Report 81-1224, 43 p.